



## 9-*cis*-UAB30, a novel rexinoid agonist, decreases tumorigenicity and cancer cell stemness of human neuroblastoma patient-derived xenografts

Raoud Marayati<sup>a</sup>, Laura V. Bownes<sup>a</sup>, Laura L. Stafman<sup>a</sup>, Adele P. Williams<sup>a</sup>, Colin H. Quinn<sup>a</sup>, Venkatram Atigadda<sup>b</sup>, Jamie M. Aye<sup>c</sup>, Jerry E. Stewart<sup>a</sup>, Karina J. Yoon<sup>d</sup>, Elizabeth A. Beierle<sup>a,\*</sup>

<sup>a</sup> Division of Pediatric Surgery, Department of Surgery, University of Alabama at Birmingham, Birmingham, AL 35233, USA

<sup>b</sup> Department of Dermatology, University of Alabama at Birmingham, Birmingham, AL 35233, USA

<sup>c</sup> Division of Pediatric Hematology Oncology, Department of Pediatrics, University of Alabama at Birmingham, Birmingham, AL 35233, USA

<sup>d</sup> Department of Pharmacology and Toxicology, University of Alabama at Birmingham, Birmingham, AL 35233, USA

### ARTICLE INFO

#### Article history:

Received 21 July 2020

Received in revised form 16 September 2020

Accepted 21 September 2020

### ABSTRACT

Retinoic acid (RA) therapy has been utilized as maintenance therapy for high-risk neuroblastoma, but over half of patients treated with RA relapse. Neuroblastoma stem cell-like cancer cells (SCLCCs) are a subpopulation of cells characterized by the expression of the cell surface marker CD133 and are hypothesized to contribute to drug resistance and disease relapse. A novel rexinoid compound, 9-*cis*-UAB30 (UAB30), was developed having the same anti-tumor effects as RA but a more favorable toxicity profile. In the current study, we investigated the efficacy of UAB30 in neuroblastoma patient-derived xenografts (PDX). Two PDXs, COA3 and COA6, were utilized and alterations in the malignant phenotype were assessed following treatment with RA or UAB30. UAB30 significantly decreased proliferation, viability, and motility of both PDXs. UAB30 induced cell-cycle arrest as demonstrated by the significant increase in percentage of cells in G1 (COA6:  $33.7 \pm 0.7$  vs.  $43.3 \pm 0.7\%$ , control vs. UAB30) and decrease in percentage of cells in S phase (COA6:  $44.7 \pm 1.2$  vs.  $38.6 \pm 1\%$ , control vs. UAB30). UAB30 led to differentiation of PDX cells, as evidenced by the increase in neurite outgrowth and mRNA abundance of differentiation markers. CD133 expression was decreased by 40% in COA6 cells after UAB30. The ability to form tumorspheres and mRNA abundance of known stemness markers were also significantly decreased following treatment with UAB30, further indicating decreased cancer cell stemness. These results provide evidence that UAB30 decreased tumorigenicity and cancer cell stemness in neuroblastoma PDXs, warranting further exploration as therapy for high-risk neuroblastoma.

### Introduction

Neuroblastoma, a tumor of neural crest origin, is the most common extracranial solid tumor in the pediatric population with over half of patients presenting with high-risk disease [1]. Tumors are considered high risk based on several factors including patient age, tumor imaging and differentiation, and *MYCN* amplification [2]. Current treatment for high-risk disease includes chemotherapy, surgical resection, autologous stem cell transplant, radiation, immunotherapy, and maintenance therapy with retinoic acid. Despite this aggressive therapeutic regimen, the survival of patients with high-risk neuroblastoma remains dismal at less than 50% [3], and over half of the children treated still relapse from drug-resistant minimal residual disease [4,5]. Stem cell-like cancer cells (SCLCCs) are a

subpopulation of cancer cells with self-renewal capacity that have been hypothesized to contribute to resistance to therapy and neuroblastoma recurrence [6,7]. Neuroblastoma SCLCCs may be recognized by the expression of the cell surface marker, CD133 [8]. Other investigators have demonstrated that CD133+ neuroblastoma cells have increased anchorage independent growth, tumorsphere formation, and proliferation [9].

13-*cis*-Retinoic acid (RA), or isotretinoin, is a differentiating agent used in maintenance therapy for high-risk neuroblastoma [2]. RA has numerous undesirable side effects, including hepatotoxicity, mucocutaneous disorders, and hypertriglyceridemia, that may limit the dosing amount and duration of treatment [10,11]. 9-*cis*-UAB30 (8-(3',4'-dihydro-1'(2'H)-naphthalen-1'-ylidene)-3,7-dimethyl-2,4,6-octatrienoic acid, UAB30) is a novel retinoid X receptor (RXR) agonist

**Abbreviations:** RA, Retinoic acid; SCLCCs, Stem cell-like cancer cells; UAB30, 9-*cis*-UAB30; PDX, Patient-derived xenografts; RXR, Retinoid X receptor; IRB, Institutional Review Board; IACUC, Institutional Animal Care and Use Committee; RPMI, Roswell Park Memorial Institute; DMSO, Dimethyl sulfoxide; PBS, Phosphate-buffered saline; APC, Allophycocyanin; IgG1, Immunoglobulin G1; ELDA, Extreme limiting dilution assay; qPCR, Real-time PCR; Oct4, Octamer-binding transcription factor 4; Sox2, Sex determining region Y-box 2; NSE, Neuron Specific Enolase; HOXC9, Homeobox C9 protein; GAP43, Growth Associated Protein 43; SEM, Standard error of the mean; ANOVA, Analysis of variance; RAR, Retinoic acid receptor; RARE, Retinoic acid response elements; CADD, Combined Annotation Dependent Depletion.

\* Corresponding author at: 1600 7th Ave. South, Lowder Building, Suite 300, University of Alabama, Birmingham, Birmingham, AL 35233, USA.

E-mail address: [elizabeth.beierle@childrens.org](mailto:elizabeth.beierle@childrens.org). (E.A. Beierle).

<http://dx.doi.org/10.1016/j.tranon.2020.100893>

1936-5233/© 2020 The Authors. Published by Elsevier Inc. on behalf of Neoplasia Press, Inc. This is an open access article under the CC BY-NC-ND license (<http://creativecommons.org/licenses/by-nc-nd/4.0/>).

that has demonstrated similar efficacy but a minimal toxicity profile when compared to RA [12,13]. Our laboratory has previously shown the effectiveness of UAB30 in long-term passage neuroblastoma cell lines in decreasing proliferation, viability, and motility *in vitro*, as well as tumor growth *in vivo* [14].

Patient-derived xenografts (PDXs) have been utilized by many investigators, and have been noted to be especially useful for drug development. The PDX model provides an opportunity to study a patient tumor *ex vivo* in order to assess the efficiency of an experimental drug while maintaining the tumor's original features [15]. Based on our previous findings of UAB30's effect on long-term passage neuroblastoma cell lines, we sought to investigate the effects of UAB30 on the malignant phenotype in PDXs. We hypothesized that UAB30 treatment would decrease cell proliferation, viability, and motility, as well as cancer cell stemness in the PDXs. We also sought to evaluate the effect of UAB30 on the CD133-enriched neuroblastoma SCLCC subpopulation.

## Methods

### Maintenance and culture of patient-derived xenografts

Two human neuroblastoma PDXs, COA3 and COA6, were developed as previously described [16]. Briefly, under Institutional Review Board and Institutional Animal Care and Use Committee approved protocols (IRB 130627006 and IACUC-09803, respectively) and following parental informed consent and patient assent, human neuroblastoma tumor specimens were obtained from pediatric patients with primary neuroblastoma undergoing surgical excision. Fresh tissue was kept in serum-free Roswell Park Memorial Institute (RPMI) 1640 medium on ice for transport to the laboratory. These specimens were then implanted with 25% Matrigel (BD Biosciences, Franklin Lakes, NJ) into the flank of athymic nude mice (Envigo, Prattville, AL). When tumors reached IACUC parameters, mice were euthanized and tumors were harvested. A portion of each tumor was then sequentially passed into another mouse to maintain the PDX line, while separate portions were dissociated using a tumor dissociation kit (Miltenyi Biotec, San Diego, CA) and used for experimentation. Both COA3 and COA6 PDXs are *MYCN* amplified tumors [17], classified as high-risk disease, and have been demonstrated to recapitulate the properties of the parent tumor after several passages [16]. Both PDXs were monitored using histologic and molecular analyses and verified within the last 12 months using short tandem repeat analysis (Heflin Center for Genomic Sciences, UAB, Birmingham, AL). In addition, real-time PCR (qPCR) was routinely performed to assess the percentage of human and mouse DNA contained in the COA3 and COA6 PDXs to ensure that the tumors did not harbor murine contamination (TRENDD RNA/DNA Isolation and TaqMan QPCR/Genotyping Core Facility, UAB, Birmingham, AL). PDX cells do not propagate in culture but are maintained in standard culture conditions at 37 °C and 5% CO<sub>2</sub> in neurobasal media (Life Technologies, Carlsbad, CA) and supplemented with B-27 supplement without Vitamin A (Life Technologies), N2 supplement (Life Technologies), amphotericin B (250 µg/mL), gentamicin (50 µg/mL), L-glutamine (2 mM), epidermal growth factor (10 ng/mL; Miltenyi Biotec), and fibroblast growth factor (10 ng/mL; Miltenyi Biotec) for experiments.

### Compounds and reagents

UAB30 (9-*cis*-UAB30), a novel rexinoid agonist, was designed and produced by our colleagues in the department of chemistry as described [18]. RA (13-*cis*-RA) was obtained from Sigma (R3255, Sigma-Aldrich, St. Louis, MO). Both compounds were diluted with dimethyl sulfoxide (DMSO). An equivalent concentration of the vehicle, DMSO, at the highest diluent concentration, was utilized as a control for all experiments, and referred to as "control".

### Cell morphology

Following dissociation, COA3 and COA6 cells ( $3 \times 10^6$ ) were plated as a single cell suspension onto low attachment 6-well plates and treated with increasing doses of RA or UAB30 (0–50 µM). After 96 h, the wells were imaged using Photometrics CoolSNAP HQ2 CCD camera (Tucson, AZ) attached to a Nikon Eclipse Ti microscope (Tokyo, Japan). Cells were assessed for morphologic changes including neurite outgrowth, a marker of differentiation [19]. Neurite outgrowth was measured using ImageJ software (Ver 1.49, <http://imagej.nih.gov/ij>) and calculated as neurite length to cell body ratio as previously described [20].

### Proliferation and viability

The CellTiter 96® assay was used to assess the effect of RA and UAB30 on proliferation in neuroblastoma PDX cells *in vitro*. Both COA3 and COA6 cells ( $1 \times 10^4$  cells/well) were plated in a 96-well plate, and treated with increasing doses of RA or UAB30 (0, 10, 25, 50, 100 µM) for 96 h. CellTiter 96® dye (10 µL, Promega, Madison, WI) was then added to each well and the absorbance was measured at 490 nm using a microplate reader (BioTek Gen5, BioTek Instruments, Winooski, VT). Similarly, COA3 or COA6 cells ( $3 \times 10^4$  cells/well) were plated in a 96-well plate to perform the alamarBlue® assay to measure viability. Cells were treated with increasing doses of RA and UAB30 (0, 10, 25, 50, 100 µM) for 96 h. AlamarBlue® dye (10 µL, Thermo Fisher Scientific, Waltham, MA) was added to each well and the absorbance at 562 nm (reduced reagent) and 595 nm (oxidized reagent) was measured using a microplate reader (BioTek Gen5).

### Migration and invasion

The effect of RA and UAB30 on migration was assessed using a modified Boyden chamber assay. For COA3 cells, following treatment with 50 µM of RA or UAB30 for 24 h,  $3 \times 10^5$  cells were seeded into 8 µm pore inserts (TransWell®, Corning, Corning, NY). Cells were allowed to migrate for 7 days with collagen type I (10 µg/mL, 100 µL) used in the outer well as a chemoattractant. For the COA6 cells,  $4 \times 10^4$  cells were seeded following treatment with 25 µM of RA or UAB30 for 24 h. Laminin (10 µg/mL, 100 µL) was employed as the chemoattractant and cells were allowed to migrate for 3 days. Inserts were fixed with 4% paraformaldehyde and stained with crystal violet and photographed. Photographs were analyzed using ImageJ software (Ver 1.49, <http://imagej.nih.gov/ij>) to quantitate migration.

Invasion was assessed in a similar fashion, except a layer of Matrigel™ (1 mg/mL, 50 µL, BD Biosciences) was used to coat the top of the insert membrane. For COA3 cells,  $3 \times 10^5$  cells were seeded following treatment with 50 µM of RA or UAB30 for 24 h, collagen was used in the outer well as a chemoattractant, and cells were allowed to invade for 7 days. For the COA6 cells,  $4 \times 10^4$  cells were seeded following treatment with 25 µM of RA or UAB30 for 24 h, laminin was employed as the chemoattractant, and cells were allowed to invade for 7 days. Inserts were then fixed with 4% paraformaldehyde and stained with crystal violet and photographed. Photographs were analyzed using ImageJ to quantitate invasion.

### Cell cycle

COA3 cells ( $3 \times 10^6$ ) were plated in a 6-well plate and treated with increasing doses of RA or UAB30 (0, 25, and 50 µM). Similarly, COA6 cells ( $3 \times 10^6$ ) were plated and treated with increasing doses of RA or UAB30 (0, 10, and 25 µM). After 24 h, cells were separated into a single cell suspension using Accutase® (Corning), washed with phosphate-buffered saline (PBS), and fixed with 100% ethanol at 4 °C for at least 30 min. Following a second wash with PBS, cells were stained with propidium iodide (Invitrogen, Carlsbad, CA), 0.1% TritonX (Active Motif, Carlsbad, CA), and RNase A (0.1 mg/mL, Qiagen, Germantown, MD), and cell cycle data were obtained using the FACSCalibur™ Flow Cytometer (BD Biosciences) and analyzed using the FlowJo software (FlowJo, LLC, Ashland, OR).

### Flow cytometry

Following treatment with increasing doses of RA or UAB30 (0, 25, 50  $\mu\text{M}$  for COA3 and 0, 10, 25  $\mu\text{M}$  for COA6) for 24 h, cells ( $3 \times 10^6$ ) were labeled with an Allophycocyanin (APC)-conjugated mouse immunoglobulin G1 (IgG1) anti-human CD133/1 (clone AC133, Miltenyi Biotec) according to the manufacturer's instructions. Unlabeled cells were used as negative controls. The percentage of cells positive for APC was determined via flow cytometry using the FACSCalibur™ Flow Cytometer (BD Biosciences) and analyzed using the FlowJo software (FlowJo, LLC), quantifying the percentage of cells positive for CD133.

### Extreme limiting dilution assay

COA3 or COA6 cells were plated in a 96-well plate with a decreasing number of cells in each row of 10 wells (5000 to 1 cells for COA3 and 1000 to 1 cells for COA6). Cells were treated with RA or UAB30 (0, 50  $\mu\text{M}$  for COA3 and 0, 25  $\mu\text{M}$  for COA6). After one week, each well was assessed for tumorsphere formation. The number of wells containing spheres were counted and data analyzed using the extreme limiting dilution assay (ELDA) software (<http://bioinf.wehi.edu.au/software/elda/>).

### Real-time PCR (qPCR)

COA3 or COA6 cells were treated with RA or UAB30 at 10 and 25  $\mu\text{M}$  for 72 h. The RNeasy kit (Qiagen) was used to extract total cellular RNA according to the manufacturer's protocol. cDNA was synthesized utilizing an iScript cDNA Synthesis kit (Bio-Rad, Hercules, CA) with 1  $\mu\text{g}$  of RNA used in a 20  $\mu\text{L}$  reaction. Resulting reverse transcription products were stored at  $-20^\circ\text{C}$  until further use. For quantitative real-time PCR, SsoAdvanced™ SYBR® Green Supermix (Bio-Rad) was utilized according to manufacturer's protocol. Primers specific for the transcription factors Octamer-binding transcription factor 4 (Oct4), homeobox protein Nanog, and sex determining region Y-box 2 (Sox2) as well as for  $\beta$ -actin were obtained from Applied Biosystems (Foster City, CA). Primers for nestin, beta 3 ( $\beta$ 3)-tubulin (encoded by TUBB3), Neuron Specific Enolase (NSE, encoded by ENO2), Homeobox C9 protein (HOXC9), and Growth Associated Protein 43 (GAP43) were designed using Primer3 web version 4.1.0 [21] and checked for non-specific binding using the basic local alignment search tool (BLAST, NCBI). Sequences for the primers are included in the Supplementary material (Supplementary Table 1). qPCR was performed with 10 ng cDNA in 20  $\mu\text{L}$  reaction volume using an Applied Biosystems 7900HT cyclor (Applied Biosystems). Cycling conditions were as follows:  $95^\circ\text{C}$  for 2 min, followed by 39-cycle amplification at  $95^\circ\text{C}$  for 5 s and  $60^\circ\text{C}$  for 30 s.  $\beta$ -actin was utilized as an internal control. Gene expression was calculated using the  $\Delta\Delta\text{Ct}$  method [22] and reported as mean fold change  $\pm$  standard error of the mean (SEM).

### Magnetic cell sorting

In order to examine potential differences in the effects of RA and UAB30 on the SCLCC subpopulation and the bulk population, PDX cells were sorted based on expression of the cell surface receptor CD133. A CD133 MicroBead Kit, magnetic sorting columns, and a MACS separator (Miltenyi Biotec) were used according to manufacturer's protocol. Briefly, cells were separated into a single cell suspension using Accutase® (Corning) and incubated with an FcR blocking reagent for 5 min prior to incubation with CD133-binding magnetic beads for 20 min at  $4^\circ\text{C}$ . Cells were then passed through a magnetic column so that CD133-depleted cells flowed through while CD133-enriched cells were bound to the column and subsequently flushed into a separate tube. Separation efficiency was determined using a check reagent and FACS analysis. This process generated subpopulations of CD133-enriched cells and CD133-depleted cells which were plated immediately for experimentation.

### Statistical analysis

All experiments were performed at a minimum of three biologic replicates. Data were reported as mean  $\pm$  SEM of separate experiments. Student's *t*-test or analysis of variance (ANOVA) was used as appropriate. Statistical significance was defined as  $p \leq 0.05$ .

## Results

### Treatment with RA and UAB30 resulted in neurite outgrowth

In culture, COA6 cells typically form tumorspheres as demonstrated in Fig. 1A, C (left panels). We analyzed COA6 cells for morphologic changes following treatment with UAB30 or RA, which is known to function as a differentiating agent in neuroblastoma [23]. Cells treated with RA began to demonstrate neurite outgrowth, a finding characteristic of cell differentiation, which was best seen starting at 25  $\mu\text{M}$  (Fig. 1A, middle and left panels, black arrows). Cells treated with UAB30 began to demonstrate neurite outgrowth at doses as low as 10  $\mu\text{M}$  (Fig. 1C, middle and left panels, black arrows). We quantified neurite outgrowth by measuring neurite length to cell body diameter ratio and found that treatment with RA ( $p \leq 0.05$ ) or UAB30 ( $p \leq 0.01$ ) resulted in a significant increase in neurite outgrowth in COA6 PDX cells (Fig. 1B, D). These findings confirmed the two compounds' effect on differentiation.

### Treatment with RA and UAB30 resulted in decreased proliferation and viability

The CellTiter 96® Assay was employed to evaluate proliferation after treatment with increasing doses of RA and UAB30 (0, 10, 25, 50, 100  $\mu\text{M}$ ). UAB30 and RA were found to have a similar effect on proliferation in the COA3 cells ( $p \leq 0.01$  for UAB30 and  $p \leq 0.05$  for RA, Fig. 2A). Proliferation in COA6 cells was significantly affected by UAB30 ( $p \leq 0.001$ ) with little effect from RA at 25 and 50  $\mu\text{M}$  ( $p \leq 0.05$ ) and no significant effect at the highest dose (Fig. 2B). The alamarBlue® assay was used to evaluate the effect of RA and UAB30 on neuroblastoma viability. Following treatment with UAB30, there was a significant decrease in viability of COA3 cells ( $p \leq 0.001$ , Fig. 1C) and a trend in decreased viability with increasing doses of RA (Fig. 1C). Treatment with UAB30 led to significantly decreased viability in COA6 cells ( $p \leq 0.001$ ), whereas RA had nominal effect on viability of COA6 cells (Fig. 2D).

### Treatment with RA and UAB30 resulted in decreased migration and invasion

The effect of RA and UAB30 on cell motility was assessed using migration and invasion assays. Since non-viable cells are not motile, COA3 and COA6 cells were treated with drug concentrations below those seen to cause significant cell death (50  $\mu\text{M}$  RA or 25  $\mu\text{M}$  UAB30, Fig. 2C, D). Both RA and UAB30 were found to significantly decrease migration in COA3 cells ( $p \leq 0.01$ , Fig. 3A). In COA6 cells, UAB30 also significantly decreased migration ( $p \leq 0.01$ ), but RA did not statistically affect migration (Fig. 3B). The invasion assay, which required cells to invade through a Matrigel™ layer prior to migrating through the insert membrane pores, demonstrated that both RA and UAB30 significantly decreased invasion in COA3 PDX cells ( $p \leq 0.01$  for RA and  $p \leq 0.001$  for UAB30, respectively, Fig. 3A). Similar to migration, treatment with UAB30 significantly decreased invasion in COA6 cells ( $p \leq 0.01$ , Fig. 3D), while RA did not result in a statistically significant change in invasion (Fig. 3D). Representative photos of the migration and invasion inserts are shown (Fig. 3A-D, panels to the right of the graphs).

### Treatment with RA and UAB30 inhibited progression through the cell cycle

Flow cytometry was used to assess the effect of RA and UAB30 on the cell cycle. COA3 and COA6 cells were treated with RA or UAB30 (25 and 50  $\mu\text{M}$  of RA or UAB30 for COA3 and 10 and 25  $\mu\text{M}$  of RA or UAB30 for COA6) and the cell cycle was analyzed after 24 h. In COA3 cells, treatment

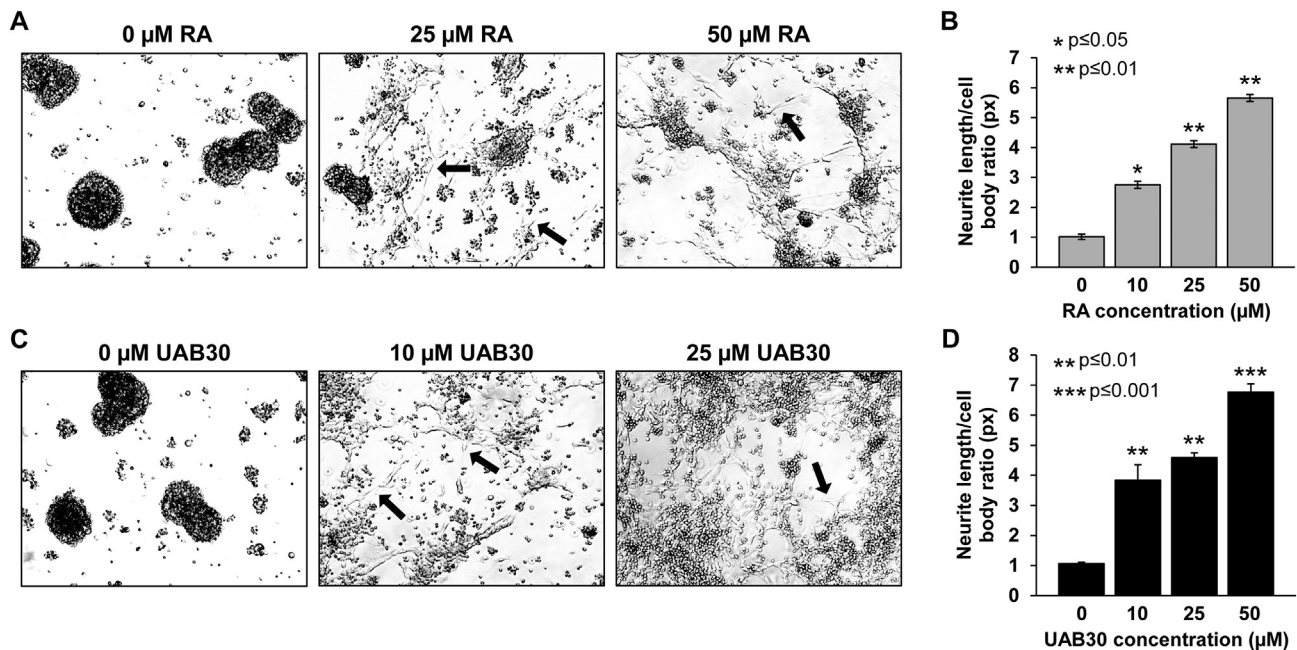


**Fig. 1.** Treatment with RA and UAB30 resulted in increased neurite outgrowth. COA6 cells were plated as a single cell suspension onto low attachment plates and treated with increasing doses (0–50 μM) of (A, B) RA or (C, D) UAB30. After 96 h, cells were imaged and assessed for neurite outgrowth, a marker of differentiation, using Photometrics CoolSNAP HQ2 CCD camera attached to a Nikon Eclipse Ti microscope. Treatment with both (A) RA and (C) UAB30 resulted in neurite outgrowth (*middle panels, black arrows*). (B, D) Neurite outgrowth was quantified by measuring neurite length to cell body diameter ratio in pixels (px) using ImageJ software.

with both RA and UAB30 led to an increase in the percentage of cells in the G1 phase and a decrease in the percentage of cells in S phase, indicating failure of cells to progress through the cell cycle and arrest in the G1 phase following treatment ( $p \leq 0.05$ , Fig. 4A). In COA6 cells, treatment with UAB30 inhibited cell-cycle progression, with an increase in the percentage of cells

in the G1 phase and a decrease in the percentage of cells in the S and G2 phase ( $p \leq 0.05$ , Fig. 4B). Treatment of COA6 cells with RA had a variable effect on the G1 and S phase with no statistically significant change (Fig. 4B). Data are presented in graphic (Fig. 4A, B) as well as tabular form with mean  $\pm$  SEM reported (Fig. 4C, D).

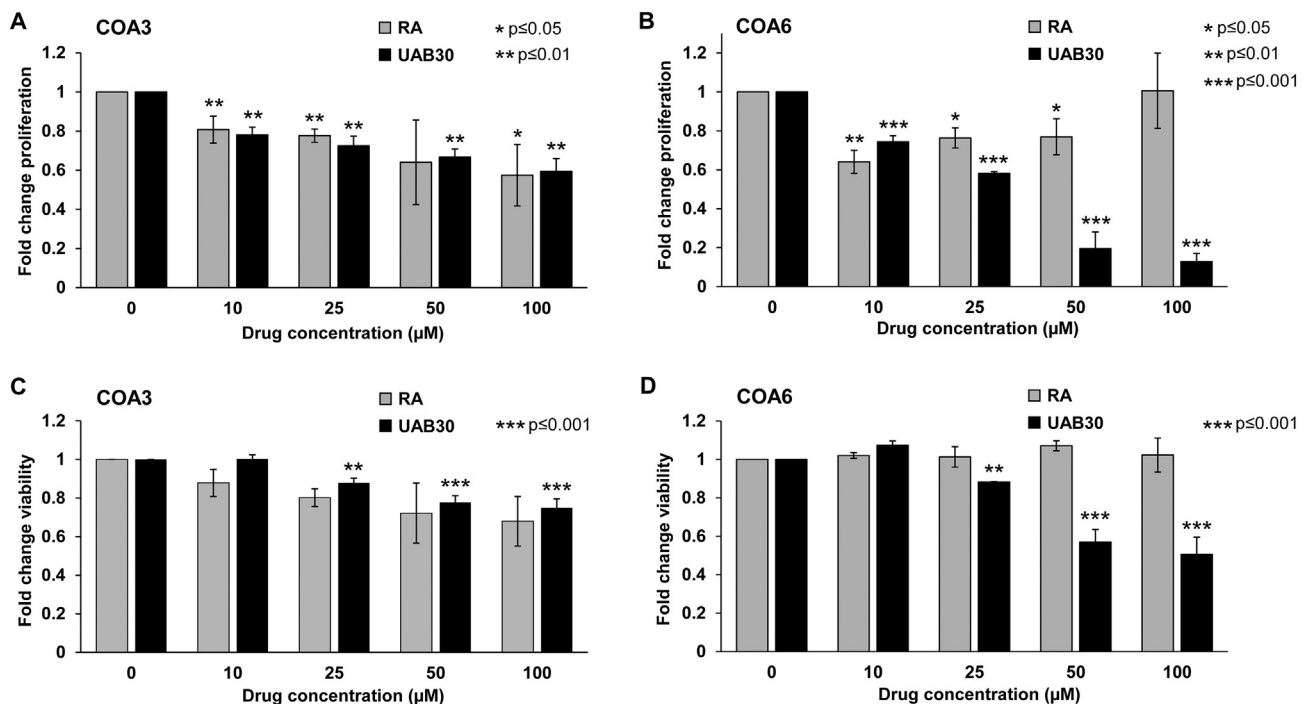


**Fig. 2.** Treatment with RA and UAB30 decreased proliferation and viability. COA3 and COA6 were treated with increasing concentrations of RA or UAB30 (0, 10, 25, 50, 100 μM) for 96 h. (A, B) Proliferation was measured using CellTiter 96® assay. Proliferation was significantly decreased after treatment with RA or UAB30 in COA3 cells. In COA6 cells, UAB30 had a more marked effect than RA, which showed no significant effect at the highest dose. (C, D) Viability was measured with alamarBlue® assay. Treatment with RA resulted in a trend towards decreased viability in COA3 with no effect on COA6 cells. Treatment with UAB30 resulted in significantly decreased cell viability in both PDXs.

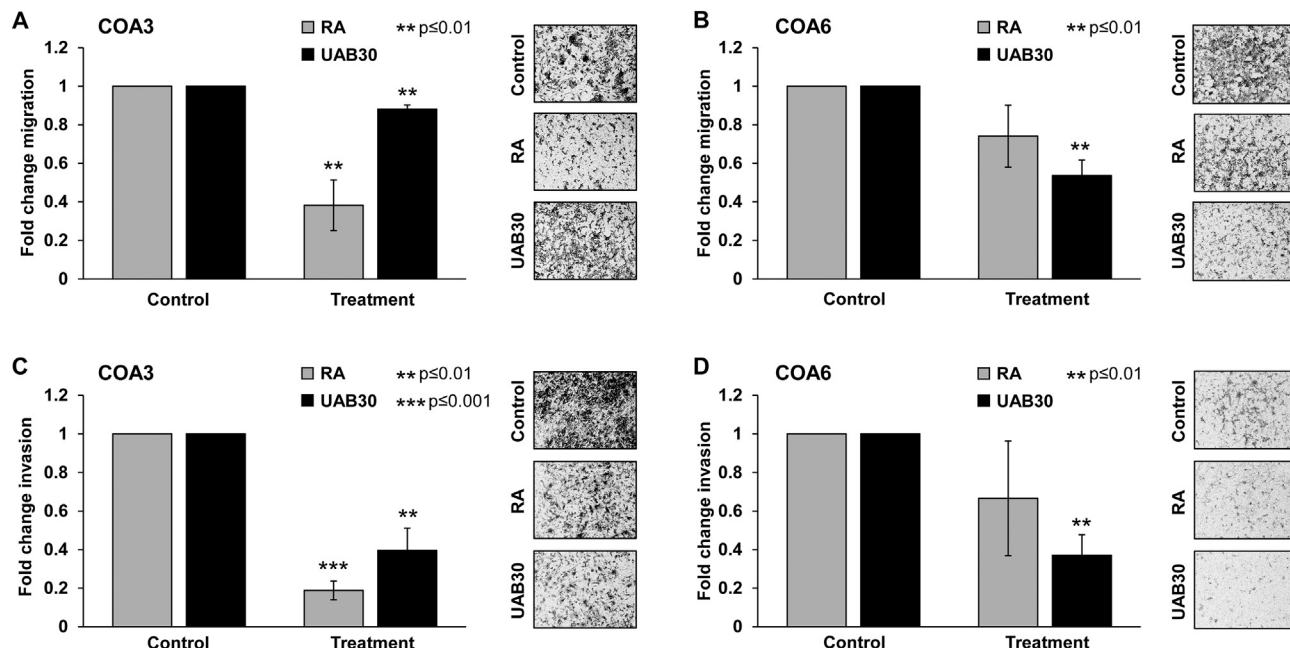
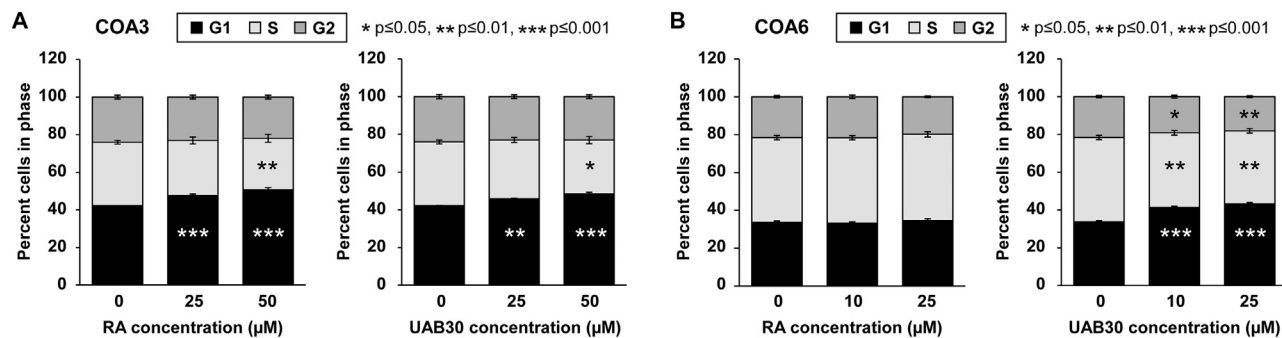


**Fig. 3.** Treatment with RA and UAB30 decreased migration and invasion. Migration and invasion were assessed following treatment with RA and UAB30. (A, B) To assess migration, COA3 cells were treated with RA and UAB at 0 or 50  $\mu\text{M}$  concentration, and COA6 cells were treated with RA and UAB at 0 or 25  $\mu\text{M}$ . COA3 ( $3 \times 10^5$ ) and COA6 ( $4 \times 10^4$ ) cells were seeded into modified Boyden chambers. Inserts were coated on the bottom with collagen for COA3 cells and with laminin for COA6 cells. COA3 cells were allowed to migrate for 7 days and COA6 cells for 3 days. Photographs of the inserts were taken with representatives shown (panels to the right of the graphs) and migration reported as mean fold change  $\pm$  standard error of the mean (SEM). (A) Treatment with RA and UAB30 significantly decreased migration in COA3 cells. (B) Only treatment with UAB30 demonstrated a significant decrease in migration of COA6 cells. (C, D) Invasion was assessed similarly with the addition of a Matrigel™ layer to the top of the insert. COA3 and COA6 cells were treated and seeded similar to previously described for migration. COA3 and COA6 cells were allowed to invade for 7 days. Photographs of the inserts were taken with representatives shown (panels to the right of the graphs) and invasion reported as mean fold change  $\pm$  SEM. (C) COA3 cells treated with RA and UAB30 had significantly decreased invasion. (D) In COA6 cells, similar to migration, only UAB30 treatment significantly decreased invasion.



COA3							
RA ( $\mu\text{M}$ )	0	25	50	UAB30 ( $\mu\text{M}$ )	0	25	50
G1	42.3 $\pm$ 0.1	47.7 $\pm$ 0.8 ***	50.7 $\pm$ 1.1 ***		42.3 $\pm$ 0.1	45.8 $\pm$ 0.3 **	48.4 $\pm$ 0.9 ***
S	33.7 $\pm$ 1.0	29.2 $\pm$ 1.8	27.3 $\pm$ 2.1 **		33.7 $\pm$ 1.0	31.2 $\pm$ 1.3	28.5 $\pm$ 1.9 *
G2	24.1 $\pm$ 1.1	23.1 $\pm$ 1.0	22.0 $\pm$ 1.0		24.1 $\pm$ 1.1	23.0 $\pm$ 1.0	23.1 $\pm$ 1.0

COA6							
RA ( $\mu\text{M}$ )	0	10	25	UAB30 ( $\mu\text{M}$ )	0	10	25
G1	33.7 $\pm$ 0.7	33.3 $\pm$ 0.6	34.6 $\pm$ 1.0		33.7 $\pm$ 0.7	41.4 $\pm$ 0.6 ***	43.3 $\pm$ 0.7 ***
S	44.7 $\pm$ 1.2	45.1 $\pm$ 1.1	45.5 $\pm$ 1.4		44.7 $\pm$ 1.2	39.5 $\pm$ 1.2 **	38.6 $\pm$ 1.2 **
G2	21.6 $\pm$ 0.6	21.7 $\pm$ 0.9	19.8 $\pm$ 0.4		21.6 $\pm$ 0.6	19.1 $\pm$ 0.7 *	18.1 $\pm$ 0.5 **

\*  $p \leq 0.05$ , \*\*  $p \leq 0.01$ , \*\*\*  $p \leq 0.001$  vs. control

**Fig. 4.** Treatment with RA and UAB30 led to failure to progress through the cell cycle. (A, C) COA3 cells ( $3 \times 10^6$ ) and (B, D) COA6 cells ( $3 \times 10^6$ ) were treated for 24 h with increasing doses of RA or UAB30 (0, 25, 50  $\mu\text{M}$  for COA3 and 0, 10, 25  $\mu\text{M}$  for COA6). Cells were stained with propidium iodide and were analyzed using FACS Flow Cytometry to evaluate the effects of RA and UAB30 on the cell cycle. FlowJo software was used for analysis. Cell cycle results shown graphically demonstrate (A) the significant increase in G1 with RA and UAB30 in COA3 cells along with a decrease in S phase at higher doses, whereas (B) a significant increase of G1 and decrease in S and G2 phases in COA6 cells was only seen with UAB30 treatment. Summary tables of the cell cycle analysis in (C) COA3 and (D) COA6 cells are provided. Data are reported as mean  $\pm$  standard error of the mean.

### Treatment with RA and UAB30 led to decreased CD133 cell surface expression

We used CD133, which has previously been identified as a cell surface marker for cell stemness in neuroblastoma [8], to evaluate the effect of RA and UAB30 on the frequency of SCLCCs. COA3 and COA6 cells were treated with RA or UAB30 for 24 h and the expression of CD133 examined using FACS. We found decreased percentage of CD133 positive COA3 cells following treatment with both RA (to  $71 \pm 5$  and  $79 \pm 7\%$  of control at 25 and 50  $\mu\text{M}$ , respectively,  $p \leq 0.05$ , Fig. 5A) and UAB30 (to  $78 \pm 7$  and  $75 \pm 8\%$  of control at 25 and 50  $\mu\text{M}$ , respectively,  $p \leq 0.05$ , Fig. 5A). In COA6 cells, UAB30 led to a significant decrease in the percentage of CD133 positive cells ( $56 \pm 13\%$  and  $46 \pm 20\%$  at 10 and 25  $\mu\text{M}$ , respectively, compared to control,  $p \leq 0.05$ , Fig. 5B), but RA did not significantly alter CD133 cell surface expression (Fig. 5B). These findings indicated a decrease in the stem-cell like phenotype.

### Treatment with RA and UAB30 led to decreased tumorsphere formation

Since CD133 expression was affected by RA and UAB30, an extreme limiting dilution assay was utilized to assess tumorsphere forming ability, which is another known characteristic of SCLCCs. PDX cells were plated in decreasing numbers (from 5000 to 1 cell per well for COA3 and from 1000 to 1 cell per well for COA6) in a 96-well plate and treated with RA or UAB30 (50  $\mu\text{M}$  for COA3 and 25  $\mu\text{M}$  for COA6). In COA3 cells, there was a significant decrease in tumorsphere formation following treatment with either RA or UAB30 ( $p < 0.001$ , Fig. 5C) indicating decreased cancer cell stemness. However, in COA6 cells, UAB30 led to a significant decrease in tumorsphere formation ( $p \leq 0.01$ , Fig. 5D), whereas RA did not significantly decrease tumorsphere formation ( $p = 0.07$ , Fig. 5D). These findings further indicated decreased cancer cell stemness in PDX cells following treatment with UAB30.

### Treatment with UAB30 led to a decrease in mRNA abundance of stem cell markers and increase in mRNA abundance of differentiation markers

Oct4, Nanog, Sox2, and nestin are known markers of neuroblastoma cancer cell stemness [7,24,25]. To evaluate the effect of UAB30, specifically, on cancer cell stemness, we measured the abundance of mRNA of these four markers using qPCR following treatment of COA3 and COA6 with UAB30 (0, 10 and 25  $\mu\text{M}$ ) for 72 h. We found that UAB30 led to significantly decreased mRNA abundance of all four markers in both COA3 ( $p \leq 0.05$ , Fig. 6A) and COA6 ( $p \leq 0.05$ , Fig. 6B) PDX cells. These data provide further evidence of UAB30 decreasing cell stemness.

$\beta$ -Tubulin, NSE, HOXC9, and GAP43, have been shown to be associated with neuroblastoma differentiation [26–29]. To evaluate the effect of UAB30 on differentiation of neuroblastoma PDXs, COA3 and COA6 were treated with UAB30 (0, 10 and 25  $\mu\text{M}$ ) for 72 h and mRNA abundance of the four differentiation markers evaluated using qPCR. Treatment with UAB30 significantly increased mRNA abundance of all four genes in both PDX cells ( $p \leq 0.05$ , Fig. 6C, D), indicating increased differentiation.

### Treatment with UAB30 decreased proliferation and viability of both CD133-enriched and CD133-depleted subpopulations

To study the effect of RA and UAB30 on SCLCCs, we isolated this subpopulation from the bulk PDX cells. Both COA3 and COA6 cells were sorted into CD133-enriched and CD133-depleted subpopulations using magnetic cell sorting. Cells were then treated with RA and UAB30 at increasing concentrations (0, 25, 50, and 100  $\mu\text{M}$  for COA3 and 0, 10, 25, 50, 100  $\mu\text{M}$  for COA6) and proliferation and viability assessed using CellTiter 96® and alamarBlue® assays, respectively.

In evaluating proliferation of sorted COA3 cells, both the CD133-enriched and CD133-depleted subpopulations were sensitive to treatment with RA and UAB30 ( $p \leq 0.05$  compared to the control bars corresponding to each

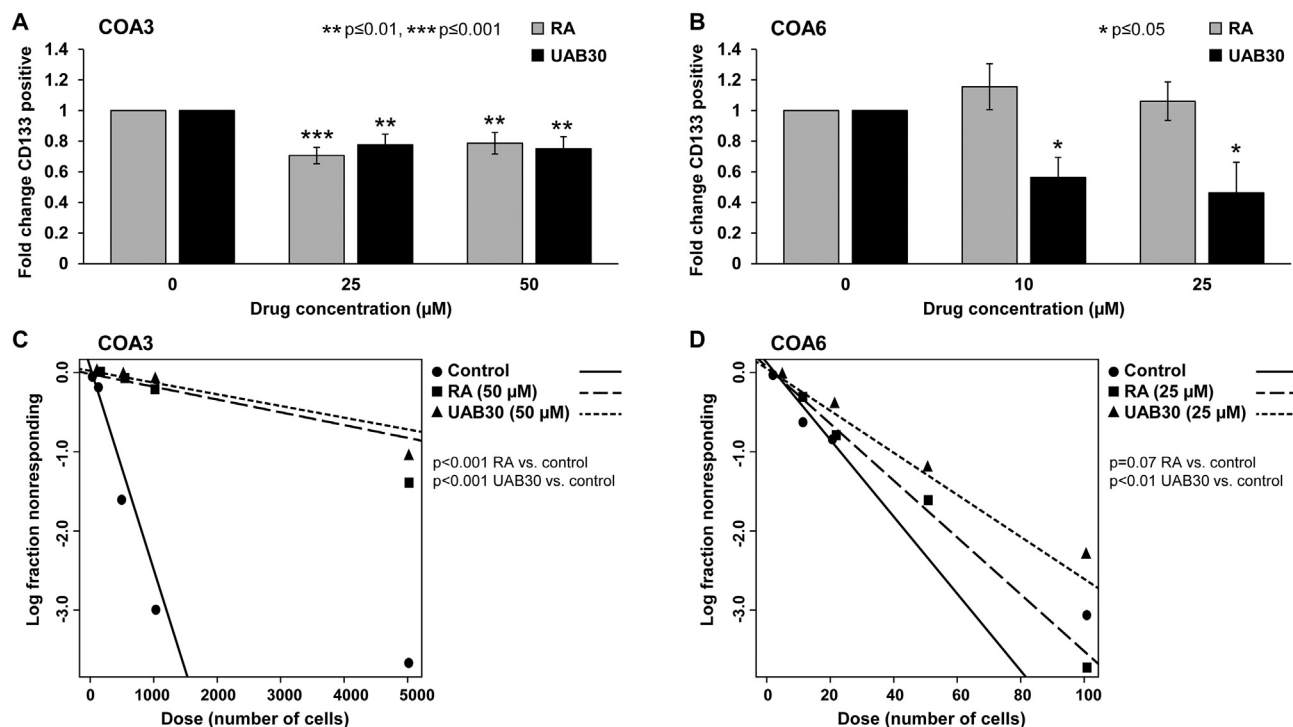


**Fig. 5.** Treatment with RA and UAB30 decreased CD133 expression and tumorsphere formation. CD133 cell surface expression was determined using flow cytometry in (A) COA3 and (B) COA6 cells following treatment with RA or UAB30 (0, 25, 50  $\mu\text{M}$  for COA3 and 0, 10, 25  $\mu\text{M}$  for COA6). (A) In COA3 cells, treatment with RA or UAB30 resulted in significantly decreased percentage of CD133 positive cells. (B) Following treatment with UAB30, COA6 cells had decreased percentage of CD133 positive cells whereas RA had no effect on CD133 cell surface expression. (C) COA3 and (D) COA6 cells were plated for an extreme limiting dilution assay with decreasing numbers of cells per well. Cells were treated with RA, or UAB30 (0, 50  $\mu\text{M}$  for COA3 and 0, 25  $\mu\text{M}$  for COA6) for one week. (C) COA3 cells treated with RA or UAB30 had significantly decreased tumorsphere formation compared to control cells. (D) Treatment with UAB30 in COA6 cells resulted in significantly decreased tumorsphere formation compared to control cells. There was a decreased tumorsphere formation in cells treated by RA, but it did not reach statistical significance.

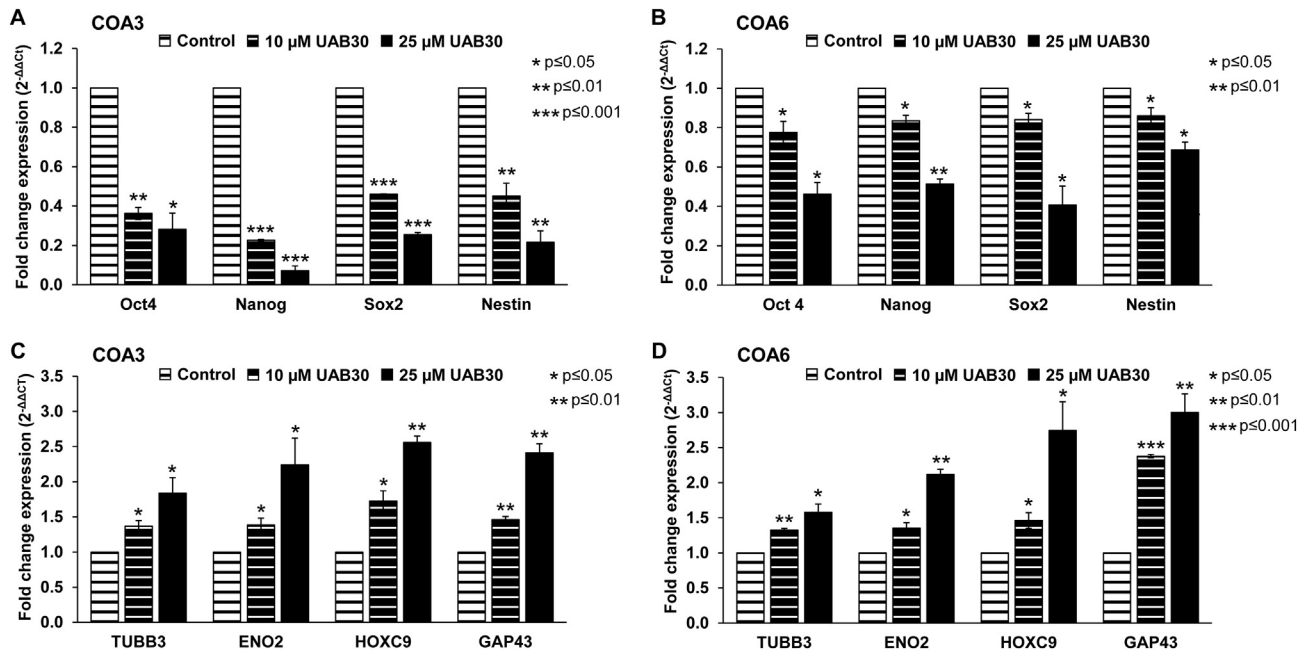


**Fig. 6.** Treatment with RA and UAB30 decreased mRNA abundance of stem cell markers and increased mRNA abundance of differentiation markers. (A) COA3 and (B) COA6 cells were treated with UAB30 (0, 10, 25 μM) for 72 h. Real-time PCR was used to examine the mRNA abundance for Oct4, Nanog, Sox2, and nestin. Gene expression was normalized to β-actin and calculated as fold change to the vehicle control using the ΔΔCt method. Treatment with UAB30 resulted in decreased mRNA of all stem cell markers in (A) COA3 and (B) COA6 cells and increased mRNA of differentiation markers in (C) COA3 and (D) COA6 cells.

subpopulation, Fig. 7A, B). However, in sorted COA6 cells, treatment with RA was able to decrease proliferation of the CD133-enriched only at the lower doses, while there was no significant effect at the higher doses suggesting

the ability of these cells to grow in the presence of RA (Fig. 7C). Treatment of COA6 cells with UAB30 resulted in significantly decreased proliferation of both CD133-enriched and CD133-depleted subpopulations (Fig. 7D).

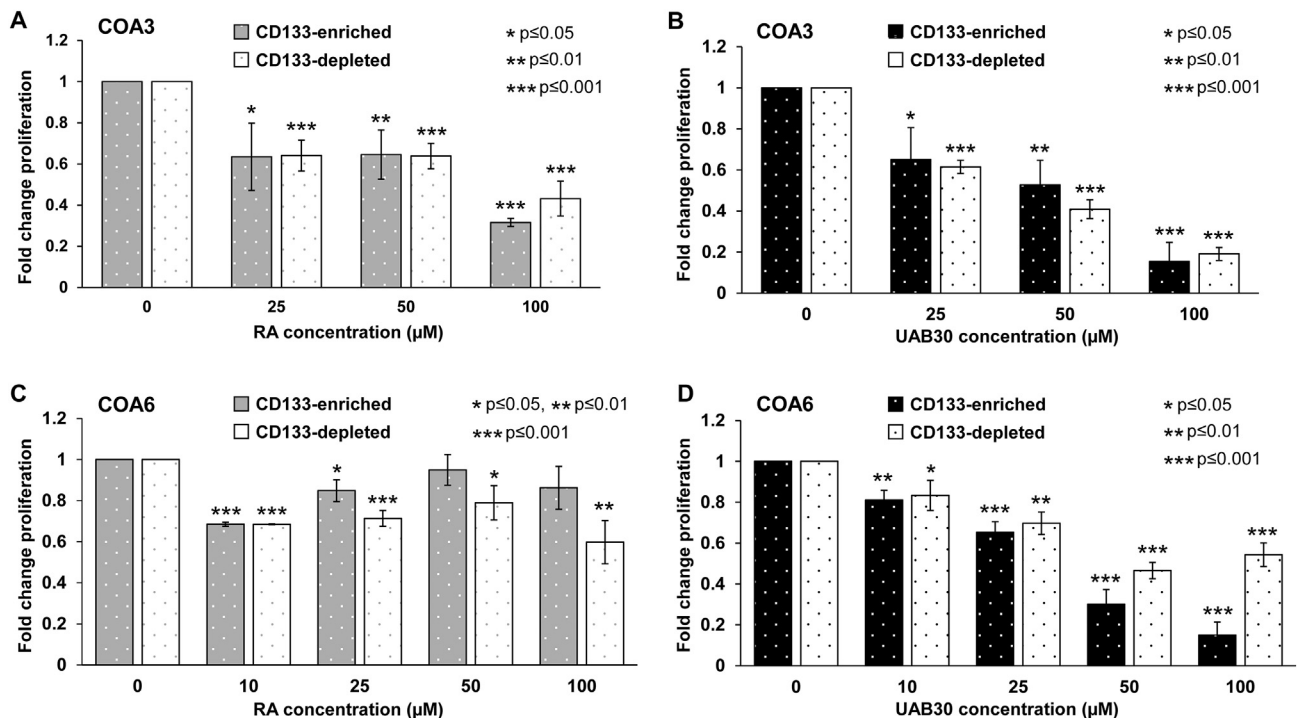


**Fig. 7.** Treatment with RA and UAB30 decreased proliferation in CD133-enriched and CD133-depleted subpopulations. (A, B) COA3 and (C, D) COA6 cells were sorted into CD133-enriched and CD133-depleted subpopulations using magnetic cell sorting, and treated with increasing doses (0, 25, 50, 100 μM) of (A, C) RA and (B, D) UAB30 for 96 h. (A, B) In sorted COA3 cells, both treatments resulted in significantly decreased proliferation in CD133-enriched and CD133-depleted subpopulations. (C) In sorted COA6 cells, RA treatment had a significant decrease in proliferation in the CD133-depleted subpopulation but not in the CD133-enriched subpopulation where there was no effect at the higher doses. (D) UAB30 treatment of sorted COA6 cells resulted in decreased proliferation in both CD133-enriched and CD133-depleted subpopulations with a more marked effect on CD133-enriched subpopulation.

Similarly in COA3 cells, treatment with RA or UAB30 led to decreased viability of both CD133-enriched and CD133-depleted subpopulations ( $p \leq 0.05$ , Fig. 8A, B). Treatment of sorted COA6 cells demonstrated that both the CD133-enriched and CD133-depleted subpopulations were sensitive to UAB30 ( $p \leq 0.05$ , Fig. 8D), whereas there was minimal change in viability of the CD133-enriched subpopulation with RA (Fig. 8C). Taken together, these results indicate that both COA3 and COA6 CD133-enriched cells were effectively targeted with UAB30.

## Discussion

In the current study, we have demonstrated that treatment with UAB30 decreased tumorigenicity and cancer cell stemness in neuroblastoma PDXs. We have previously demonstrated similar results when utilizing long-term passage neuroblastoma cell lines [14]. However, the use of the two PDXs, which have been shown to recapitulate the architecture and characteristics of the parent neuroblastoma tumors [16], provided a unique opportunity for pre-clinical evaluation of novel therapeutics and made this study innovative. We utilized xenografts from two different patients with *MYCN* amplified neuroblastoma [17], which has been shown to be indicative of poor prognosis and represents high-risk disease. The importance of *MYCN* amplification in the pathogenesis of high-risk neuroblastoma makes it critical that the effects seen with UAB30 treatment in *MYCN*-amplified long-term passage cell lines [14] hold true in PDXs, as was demonstrated in this study.

RA is currently included in high-risk disease treatment which is why we chose to utilize it as a comparison with UAB30 in the current study. RA binds to the retinoic acid receptor (RAR) forming a functional heterodimer with the RXR receptor that binds to the retinoic acid response elements (RARE) in the nucleus, resulting in changes in gene transcription. UAB30 selectively binds the RXR receptor, which forms a homodimer that binds the RARE regulating genes involved in differentiation and apoptosis. While both RA and UAB30 have been shown to be equally effective in neuroblastoma cell lines [14], we found varying degrees of sensitivities of

neuroblastoma PDXs to the two compounds. For example, both RA and UAB30 decreased proliferation and viability of COA3 cells. In contrast, in COA6 cells, RA had no effect on proliferation or viability even at higher doses, possibly mirroring the variable responses to therapy seen in some high-risk tumors. However, UAB30 significantly decreased proliferation and viability of COA6 cells. The premise for the use of this novel retinoid receptor agonist, UAB30, as potential therapy in neuroblastoma relies not only upon the significant anti-tumor effects seen in the current study, but upon its significantly improved side effect profile compared to RA [12]. In addition, when compared to other RXR agonists, UAB30 has high specificity for the RXR receptor without signaling through RXR:RXR (liver X receptor) or other RXR heterodimers, thus eliminating the marked hypertriglyceridemia which is the rate-limiting toxicity of bexarotene, the only FDA approved retinoid.

We speculate that potential differences in patient clinical features and as well as difference in gene expression patterns between the two PDXs may contribute to the differential response and resistance to RA. Although both PDXs were derived at initial diagnosis prior to any treatment from patients older than 18 months with high-risk characteristics including unfavorable histology and *MYCN* amplification, the two patients required variable induction regimens and conditioning prior to autologous stem cell transplant, which was then followed by RA and immunotherapy as part of their post-consolidation or maintenance therapy. In addition, whole exome sequencing of both PDXs identified fifteen coding mutations exclusive to COA6, 5 of which with a Combined Annotation Dependent Deletion (CADD) score  $\geq 20$  [17], indicating top 1% deleterious variants in the human genome. These included *CDK5RAP2*, a gene required for spindle checkpoint function. Mutation of *CDK5RAP2* has been previously thought to confer resistance to chemotherapy. Zhang et al. demonstrated that *CDK5RAP2*-knockdown cells have increased resistance to paclitaxel and doxorubicin which is subsequently rescued by *CDK5RAP2* expression [30]. Other investigators have utilized PDXs to examine drug resistance in melanoma and identify novel therapeutic strategies against drug-resistant disease [31,32]. This report and those of other investigators

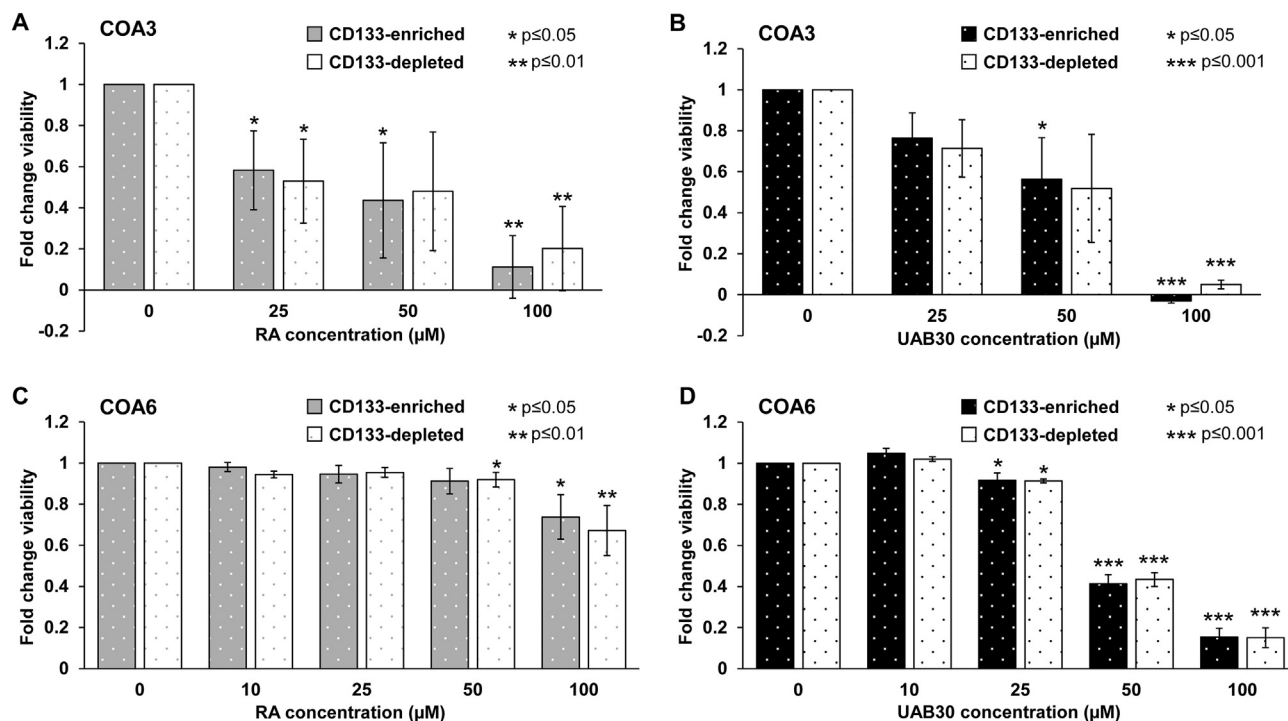


**Fig. 8.** Treatment with RA and UAB30 decreased viability in CD133-enriched and CD133-depleted subpopulations. (A, B) COA3 and (C, D) COA6 cells were sorted into CD133-enriched and CD133-depleted subpopulations using magnetic cell sorting, and treated with increasing doses (0, 25, 50, 100  $\mu\text{M}$ ) of (A, C) RA and (B, D) UAB30 for 96 h. (A, B) In sorted COA3 cells, both treatments resulted in significantly decreased viability in CD133-enriched and CD133-depleted subpopulations. (C) RA treatment of sorted COA6 cells led to a minimal change in viability of the CD133-enriched subpopulation and a decrease in viability of the CD133-depleted subpopulation at the higher doses. (D) UAB30 treatment of sorted COA6 cells decreased viability significantly in both CD133-enriched and CD133-depleted subpopulations.

highlight the important role of PDXs in modeling treatment failure in patients and disease relapse compared to conventional cell lines, which are less predictive of the effects of targeted therapies and may lose drug resistance mechanisms [33].

Cellular motility is known to correlate with the invasive capacity of human neuroblastoma cells [34]. We found that treatment with UAB30 significantly reduced migration and invasion of both neuroblastoma PDX cells whereas RA only had a significant effect on motility of COA3 cells. RA has been previously shown to decrease migration and invasiveness of neuroblastoma cells [14]. Although the mechanism is still unclear, it has been hypothesized that microtubule proteins may be involved. Messi et al. found that treatment with RA downregulated doublecortin, a microtubule-associated protein involved in neuronal migration, in the SK-N-SH neuroblastoma cell line [35]. However, cells that escaped RA treatment retained their expression of doublecortin and showed high migration and invasion capabilities [35]. In breast cancer cells, Src was identified as an off-target of two RXR agonists, UAB30 and Targretin, regulating extracellular matrix molecules and cell motility [36]. Defining the exact mechanism by which UAB30 affected neuroblastoma motility is the subject of current and future investigations.

The relation between cellular differentiation and the cell cycle has been shown in many systems, including the nervous system [37]. The determination of cells to differentiate is commonly made in the G1 phase of the cell cycle, and cell-cycle arrest is believed to be required for the induction of differentiation [38,39]. Retinoids, and particularly RA, have been shown to affect cell-cycle progression in a variety of cancer cell lines [40–43] including neuroblastoma [44–46]. UAB30 has also been shown to induce G0/G1 cell-cycle arrest in rhabdomyosarcoma [47], hepatoblastoma [48], and neuroblastoma [13,14] cell lines. In this study, we showed that treatment of COA3 with RA and both PDXs with UAB30 caused a dose-dependent block in the G1/S transition triggering a decreased S phase and an increased percentage of cells in the G1 phase, a critical stage for cell differentiation and maturation. When examined for morphologic characteristics indicative of cell differentiation, COA6 cells treated with UAB30 demonstrated neurite outgrowth at doses as low as 10  $\mu$ M. These findings of differentiation may be coupled with the lack of progression through the cell cycle. Similar results have been described by other investigators evaluating UAB30 in PDXs. Garner et al. reported cell-cycle arrest and differentiation of medulloblastoma PDX following treatment with UAB30 [49].

Neuroblastoma is believed to be a malignancy involving various degrees of block in differentiation of neural crest cells [50], with high-risk and aggressive tumors having a greater percentage of SCLCCs [51,52]. Investigators have shown that activation of RAR/RXR receptors upregulated transcription of genes involved in differentiation [53], and downregulated transcription of genes responsible for generation and maintenance of SCLCCs [54]. In preclinical studies, RA was reported to reduce stemness characteristics in various tumors including neuroblastoma [55]. Despite the clinical effectiveness of RA therapy for some neuroblastoma patients with minimal residual disease, there are still many high-risk and advanced neuroblastoma patients with tumors that do not respond to RA [56,57]. In this study, we found that treatment with RA led to decreased stemness of COA3 but not COA6 PDX cells. Conversely, we found that UAB30 treatment in both PDXs led to a significant decrease in stemness, as seen by decreased CD133 cell surface expression, tumorsphere formation, and mRNA abundance of transcription factors Oct4, Nanog, and Sox2, and neural progenitor marker nestin, all known markers of SCLCCs in neuroblastoma [7,24] associated with a more immature and aggressive cell phenotype [58–60]. In addition, UAB30 treatment resulted in a significant increase in mRNA abundance of  $\beta$ 3-tubulin, NSE, HOXC9, and GAP43, which are all genes shown to be involved in neural differentiation [26–29]. The effect of UAB30 on decreasing stemness, which lends it potentially useful in treatment of aggressive and high-risk disease, has not yet been reported in neuroblastoma.

We postulate that the failure of some patients to respond to RA may be due to the ability of the SCLCC subpopulation to escape RA therapy.

Previous studies of neuroblastoma have shown SCLCCs to be resistant to conventional therapeutic approaches [61], and patients whose tumors contained a higher percentage of this subpopulation had increased relapse [62]. This subpopulation expressed CD133 [61,62], and CD133 has been shown to be an independent predictor of worse survival in neuroblastoma patients [63]. Higher CD133 expression in neuroblastoma cells has also been associated with resistance to traditional chemotherapeutic agents *in vitro*. CD133-enriched neuroblastoma cells were more resistant to cisplatin, carboplatin, doxorubicin, and etoposide than their CD133-depleted counterparts [63,64]. Utilizing CD133 expression to separate the two neuroblastoma PDXs into CD133-enriched and CD133-depleted subpopulations allowed us to better investigate the effect of RA and UAB30 on SCLCCs. We found that CD133-enriched cells isolated from the COA6 neuroblastoma PDX exhibited significant resistance to RA compared to CD133-depleted cells. While lower doses of RA resulted in decreased proliferation of COA6 CD133-enriched cells, the ability of this CD133-enriched subpopulation to proliferate in the presence of high doses of RA, for example, might explain the minimal effect seen on the proliferation of bulk COA6 cells treated with RA. Seeing an effect on CD133-depleted but not CD133-enriched subpopulations with RA is where current therapies for neuroblastoma stand [65–67]. In contrast, treatment with UAB30 decreased proliferation and viability of both CD133-enriched and CD133-depleted cells and effectively targeted the SCLCC subpopulation that showed resistance to RA. With cure rates as low as 10% for relapsed and refractory disease [68], patients with high-risk neuroblastoma are in need of novel therapies that not only arrest growth and induce differentiation, but potentially target the cancer cells that are most resistant to treatment and that subsequently contribute to relapse. The inability of the SCLCC subpopulation to evade UAB30 makes it a promising therapeutic strategy for further exploration for high-risk neuroblastoma patients with disease relapse following treatment with RA.

Although superior to cell lines in mimicking intra- and inter-tumoral heterogeneity, certain limitations to the use of PDX models must be recognized including: (i) the use of immunocompromised animals, thus eliminating potential immune-mediated anti-tumor effects [69]; (ii) the sampling error that may occur with selection of the piece of the original tumor to implant into a mouse initially or during passage [33]; and (iii) the frequent surveillance needed to maintain authenticity [70]. Dependence on the ability of a given tumor to propagate and the often extended time required for engraftment and formation of a palpable tumor that may be then available for experimentation are other limitations [33]. Implanted COA3 and COA6 often require up to 6 months to grow. Additionally, since implantation employs minced chunks of PDX tumors and not single cell suspensions, accurately quantifying the number of cells injected is not possible. These two requirements rendered the evaluation of UAB30 on these PDXs *in vivo* unfeasible. Despite these limitations, the *in vitro* use of dissociated PDX cells extends the application of PDX models and provides a renewable source of cancer cells for experimentation while maintaining the important principles of the 3Rs (Replacement, Reduction, and Refinement) to minimize animal use.

## Conclusions

In the current study, we demonstrated that treatment with UAB30 led to a significant decrease in proliferation, viability, and motility of two high-risk neuroblastoma PDXs. UAB30, a novel rexinoid agonist, led to alterations in the malignant phenotype including inducing differentiation, inhibiting cell-cycle progression, and decreasing cancer cell stemness as shown by decreased CD133 expression, decreased tumorsphere formation, and decreased mRNA abundance of known stemness markers. In addition, treatment with UAB30 demonstrated efficacy on the CD133-enriched stem cell-like subpopulation, which may contribute to resistance to RA therapy and disease relapse. These results warrant further exploration of UAB30 as potential therapy for high-risk neuroblastoma.

Supplementary data to this article can be found online at <https://doi.org/10.1016/j.tranon.2020.100893>.

## Declaration of competing interest

The authors declare that they have no known competing financial interests or personal relationships that could have appeared to influence the work reported in this paper.

## Acknowledgements

This project was made possible by funding from the National Cancer Institute of the National Institutes of Health under award numbers T32 CA229102 (R.M. and L.V.B.); T32 CA091078 (L.L.S.); T32 CA183926 (A.P.W.); and 5T32GM008361 (C.H.Q.). The content is solely the responsibility of the authors and does not necessarily represent the official views of the National Institutes of Health. Other funding sources include Sid Strong Foundation, Elaine Roberts Foundation, Open Hands Overflowing Hearts, and Starr Fund-Vince Lombardi Cancer Foundation (E.A.B.). The authors wish to thank Vidya Sagar Hanumanthu and the UAB Comprehensive Flow Cytometry Core (P30 AI27667), and Dr. Anita Hjelmeland's laboratory for their assistance with the qPCR.

## Ethical approval statement

This study is approved by the Institutional Review Board (IRB 130627006) and the Institutional Animal Care and Use Committee (IACUC-09803) protocols.

## CRediT authorship contribution statement

Raoud Marayati: Investigation, Validation, Formal analysis, Writing - Original Draft, Writing - Review & Editing, Visualization; Laura V. Bownes: Investigation, Formal analysis, Writing - Original Draft, Writing - Review & Editing; Laura L. Stafman: Conceptualization, Methodology, Investigation, Validation, Formal analysis; Adelle P. Williams: Investigation, Validation, Formal analysis; Colin H. Quinn: Investigation, Formal analysis; Venkatram Atigadda: Resources; Jamie M. Aye: Resources; Jerry E. Stewart: Data Curation, Investigation, Formal analysis, Project administration; Karina J. Yoon: Resources; Elizabeth A. Beierle: Conceptualization, Methodology, Supervision, Funding acquisition, Writing - Review & Editing.

## References

- [1] I.V. Kholodenko, D.V. Kalinsky, Deyev S.M. Doronin II, R.V. Kholodenko, Neuroblastoma origin and therapeutic targets for immunotherapy, *J Immunol Res.* 2018 (2018), 7394268.
- [2] Smith V, Foster J. High-Risk Neuroblastoma Treatment Review. *Children (Basel)*. 2018; 5.
- [3] V.P. Tolbert, K.K. Matthay, Neuroblastoma: clinical and biological approach to risk stratification and treatment, *Cell Tissue Res.* 372 (2018) 195–209.
- [4] B.B. Cheung, Combination therapies improve the anticancer activities of retinoids in neuroblastoma, *World J Clin Oncol.* 6 (2015) 212–215.
- [5] N.O. Basta, G.C. Halliday, G. Makin, J. Birch, R. Feltbower, N. Bown, et al., Factors associated with recurrence and survival length following relapse in patients with neuroblastoma, *Br. J. Cancer* 115 (2016) 1048–1057.
- [6] X. Jin, X. Jin, H. Kim, Cancer stem cells and differentiation therapy, *Tumour Biol.* 39 (2017) (1010428317729933).
- [7] H.F. Bahmad, F. Chamaa, S. Assi, R.M. Chalhoub, T. Abou-Antoun, W. Abou-Kheir, Cancer stem cells in neuroblastoma: expanding the therapeutic frontier, *Front. Mol. Neurosci.* 12 (2019) 131.
- [8] T. Kamijo, Role of stemness-related molecules in neuroblastoma, *Pediatr. Res.* 71 (2012) 511–515.
- [9] Garner EF, Beierle EA. Cancer stem cells and their interaction with the tumor microenvironment in neuroblastoma. *Cancers (Basel)*. 2015;8.
- [10] F. Stevison, J. Jing, S. Tripathy, N. Isoherranen, Role of retinoic acid-metabolizing cytochrome P450s, CYP26, in inflammation and cancer, *Adv. Pharmacol.* 74 (2015) 373–412.
- [11] M. David, E. Hodak, N.J. Lowe, Adverse effects of retinoids, *Med Toxicol Adverse Drug Exp.* 3 (1988) 273–288.
- [12] J.M. Kolesar, R. Hoel, M. Pomplun, T. Havighurst, J. Stublaski, B. Wollmer, et al., A pilot, first-in-human, pharmacokinetic study of 9cUAB30 in healthy volunteers, *Cancer Prev. Res. (Phila.)* 3 (2010) 1565–1570.
- [13] C.F. Chou, Y.H. Hsieh, C.J. Grubbs, V.R. Atigadda, J.A. Mobley, R. Dummer, et al., The retinoid X receptor agonist, 9-cis UAB30, inhibits cutaneous T-cell lymphoma proliferation through the SKP2-p27kip1 axis, *J. Dermatol. Sci.* 90 (2018) 343–356.

- [14] A.M. Waters, J.E. Stewart, V.R. Atigadda, E. Mroczek-Musulman, D.D. Muccio, C.J. Grubbs, et al., Preclinical evaluation of a novel RXR agonist for the treatment of neuroblastoma, *Mol. Cancer Ther.* 14 (2015) 1559–1569.
- [15] A. Kamili, A.J. Gifford, N. Li, C. Mayoh, S.O. Chow, T.W. Failes, et al., Accelerating development of high-risk neuroblastoma patient-derived xenograft models for preclinical testing and personalised therapy, *Br. J. Cancer* 122 (2020) 680–691.
- [16] L.L. Stafman, A.P. Williams, R. Marayati, J.M. Aye, H.R. Markert, E.F. Garner, et al., Focal adhesion kinase inhibition contributes to tumor cell survival and motility in neuroblastoma patient-derived xenografts, *Sci. Rep.* 9 (2019) 13259.
- [17] A.L. Miller, P.L. Garcia, J.G. Pressey, E.A. Beierle, D.R. Kelly, D.K. Crossman, et al., Whole exome sequencing identified sixty-five coding mutations in four neuroblastoma tumors, *Sci. Rep.* 7 (2017) 17787.
- [18] P.T. Vedell, Y. Lu, C.J. Grubbs, Y. Yin, H. Jiang, K.I. Bland, et al., Effects on gene expression in rat liver after administration of RXR agonists: UAB30, 4-methyl-UAB30, and Targretin (bexarotene), *Mol. Pharmacol.* 83 (2013) 698–708.
- [19] J.A. Robson, N. Sidell, Ultrastructural features of a human neuroblastoma cell line treated with retinoic acid, *Neuroscience*. 14 (1985) 1149–1162.
- [20] J.A. Harrill, T.M. Freudenrich, D.W. Machacek, S.L. Stice, W.R. Mundy, Quantitative assessment of neurite outgrowth in human embryonic stem cell-derived hN2 cells using automated high-content image analysis, *Neurotoxicology*. 31 (2010) 277–290.
- [21] S. Rozen, H. Skaletsky, Primer3 on the WWW for general users and for biologist programmers, *Methods Mol. Biol.* 132 (2000) 365–386.
- [22] J. Winer, C.K. Jung, I. Shackel, P.M. Williams, Development and validation of real-time quantitative reverse transcriptase-polymerase chain reaction for monitoring gene expression in cardiac myocytes in vitro, *Anal. Biochem.* 270 (1999) 41–49.
- [23] C.P. Reynolds, Differentiating agents in pediatric malignancies: retinoids in neuroblastoma, *Curr. Oncol. Rep.* 2 (2000) 511–518.
- [24] T.C. Newton, K. Wolcott, S.S. Roberts, Comparison of the side populations in pretreatment and postrelapse neuroblastoma cell lines, *Transl. Oncol.* 3 (2010) 246–251.
- [25] J. Neradil, R. Veselska, Nestin as a marker of cancer stem cells, *Cancer Sci.* 106 (2015) 803–811.
- [26] E. Draberova, Z. Lukas, D. Ivanyi, V. Viklicky, P. Draber, Expression of class III beta-tubulin in normal and neoplastic human tissues, *Histochem. Cell Biol.* 109 (1998) 231–239.
- [27] N. Chaudhari, P. Talwar, C. Lefebvre D'hellencourt, P. Ravanan, CDDO and ATRA instigate differentiation of IMR32 human neuroblastoma cells, *Front. Mol. Neurosci.* 10 (2017) 310.
- [28] L. Mao, J. Ding, Y. Zha, L. Yang, B.A. McCarthy, W. King, et al., HOXC9 links cell-cycle exit and neuronal differentiation and is a prognostic marker in neuroblastoma, *Cancer Res.* 71 (2011) 4314–4324.
- [29] E. Ortoft, S. Pahlman, G. Andersson, V. Parrow, C. Betsholtz, U. Hammerling, Human GAP-43 gene expression: multiple start sites for initiation of transcription in differentiating human neuroblastoma cells, *Mol. Cell. Neurosci.* 4 (1993) 549–561.
- [30] X. Zhang, D. Liu, S. Lv, H. Wang, X. Zhong, B. Liu, et al., CDK5RAP2 is required for spindle checkpoint function, *Cell Cycle* 8 (2009) 1206–1216.
- [31] M. Das Thakur, F. Salangsang, A.S. Landman, W.R. Sellers, N.K. Pryer, M.P. Levesque, et al., Modelling vemurafenib resistance in melanoma reveals a strategy to forestall drug resistance, *Nature*. 494 (2013) 251–255.
- [32] M.R. Girotti, F. Lopes, N. Preece, D. Niculescu-Duvaz, A. Zambon, L. Davies, et al., Paradox-breaking RAF inhibitors that also target SRC are effective in drug-resistant BRAF mutant melanoma, *Cancer Cell* 27 (2015) 85–96.
- [33] N. Braekvelde, D. Bexell, Patient-derived xenografts as preclinical neuroblastoma models, *Cell Tissue Res.* 372 (2018) 233–243.
- [34] Y. Zaizen, S. Taniguchi, S. Suita, The role of cellular motility in the invasion of human neuroblastoma cells with or without N-myc amplification and expression, *J. Pediatr. Surg.* 33 (1998) 1765–1770.
- [35] E. Messi, M.C. Florian, C. Caccia, M. Zanisi, R. Maggi, Retinoic acid reduces human neuroblastoma cell migration and invasiveness: effects on DCX, LIS1, neurofilaments-68 and vimentin expression, *BMC Cancer* 8 (2008) 30.
- [36] M.S. Kim, D.Y. Lim, J.E. Kim, H. Chen, R.A. Lubet, Z. Dong, et al., Src is a novel potential off-target of RXR agonists, 9-cis-UAB30 and Targretin, in human breast cancer cells, *Mol. Carcinog.* 54 (2015) 1596–1604.
- [37] T. Edlund, T.M. Jessell, Progression from extrinsic to intrinsic signaling in cell fate specification: a view from the nervous system, *Cell*. 96 (1999) 211–224.
- [38] S. Ohnuma, A. Philpott, W.A. Harris, Cell cycle and cell fate in the nervous system, *Curr. Opin. Neurobiol.* 11 (2001) 66–73.
- [39] L. Zhu, A.I. Skoultschi, Coordinating cell proliferation and differentiation, *Curr. Opin. Genet. Dev.* 11 (2001) 91–97.
- [40] K. Naka, H. Yokozaki, T. Domen, K. Hayashi, H. Kuniyasu, W. Yasui, et al., Growth inhibition of cultured human gastric cancer cells by 9-cis-retinoic acid with induction of cdk inhibitor Waf1/Cip1/p21 protein, *Differentiation*. 61 (1997) 313–320.
- [41] D. Zhang, S. Vuocolo, V. Masciullo, T. Sava, A. Giordano, D.R. Soprano, et al., Cell cycle genes as targets of retinoid induced ovarian tumor cell growth suppression, *Oncogene*. 20 (2001) 7935–7944.
- [42] Q. Chen, A.C. Ross, Retinoic acid regulates cell cycle progression and cell differentiation in human monocytic THP-1 cells, *Exp. Cell Res.* 297 (2004) 68–81.
- [43] A. Shilkaitis, A. Green, K. Christov, Retinoids induce cellular senescence in breast cancer cells by RAR-beta dependent and independent pathways: potential clinical implications (review), *Int. J. Oncol.* 47 (2015) 35–42.
- [44] D. Di Martino, C. Avignolo, B. Marsano, A. Di Vinci, A. Cara, W. Giaretti, et al., Neurite outgrowth and cell cycle kinetic changes induced by cis-diamminedichloroplatinum II and retinoic acid in a human neuroblastoma cell line, *Cancer Lett.* 52 (1990) 101–106.
- [45] L.J. Wainwright, A. Lasorella, A. Iavarone, Distinct mechanisms of cell cycle arrest control the decision between differentiation and senescence in human neuroblastoma cells, *Proc. Natl. Acad. Sci. U. S. A.* 98 (2001) 9396–9400.

- [46] J. Cuende, S. Moreno, J.P. Bolanos, A. Almeida, Retinoic acid downregulates Rae1 leading to APC(Cdh1) activation and neuroblastoma SH-SY5Y differentiation, *Oncogene*. 27 (2008) 3339–3344.
- [47] A.P. Williams, A.M. Waters, J.E. Stewart, V.R. Atigadda, E. Mroczek-Musulman, D.D. Muccio, et al., A novel retinoid X receptor agonist, UAB30, inhibits rhabdomyosarcoma cells in vitro, *J. Surg. Res.* 228 (2018) 54–62.
- [48] A.M. Waters, J.E. Stewart, V.R. Atigadda, E. Mroczek-Musulman, D.D. Muccio, C.J. Grubbs, et al., Preclinical evaluation of UAB30 in pediatric renal and hepatic malignancies, *Mol. Cancer Ther.* 15 (2016) 911–921.
- [49] E.F. Garner, L.L. Stafman, A.P. Williams, J.M. Aye, C. Goolsby, V.R. Atigadda, et al., UAB30, a novel RXR agonist, decreases tumorigenesis and leptomeningeal disease in group 3 medulloblastoma patient-derived xenografts, *J. Neuro-Oncol.* 140 (2018) 209–224.
- [50] Tee A, Marshall G, Liu P, Liu T. Neuroblastoma: a malignancy due to cell differentiation block. Neuroblastoma-present and future Available from: <http://www.intechopen.com/books/neuroblastoma-present-and-future/neuroblastoma-a-malignancy-dueto-cell-differentiation-block>: INTECH Open Access Publisher. 2012:79–84.
- [51] N. Ikegaki, H. Shimada, A.M. Fox, P.L. Regan, J.R. Jacobs, S.L. Hicks, et al., Transient treatment with epigenetic modifiers yields stable neuroblastoma stem cells resembling aggressive large-cell neuroblastomas, *Proc. Natl. Acad. Sci. U. S. A.* 110 (2013) 6097–6102.
- [52] L.L. Wang, R. Suganuma, N. Ikegaki, X. Tang, A. Naranjo, P. McGrady, et al., Neuroblastoma of undifferentiated subtype, prognostic significance of prominent nucleolar formation, and MYC/MYCN protein expression: a report from the Children's Oncology Group, *Cancer*. 119 (2013) 3718–3726.
- [53] G. Giannini, M.I. Dawson, X. Zhang, C.J. Thiele, Activation of three distinct RXR/RAR heterodimers induces growth arrest and differentiation of neuroblastoma cells, *J. Biol. Chem.* 272 (1997) 26693–26701.
- [54] H.F. Bahmad, H. Samman, A. Monzer, O. Hadadeh, K. Cheaito, R. Abdel-Samad, et al., The synthetic retinoid ST1926 attenuates prostate cancer growth and potentially targets prostate cancer stem-like cells, *Mol. Carcinog.* 58 (2019) 1208–1220.
- [55] B.T. Craig, E.J. Rellinger, A.L. Alvarez, H.L. Dusek, J. Qiao, D.H. Chung, Induced differentiation inhibits sphere formation in neuroblastoma, *Biochem. Biophys. Res. Commun.* 477 (2016) 255–259.
- [56] C.P. Reynolds, K.K. Matthay, J.G. Villablanca, B.J. Maurer, Retinoid therapy of high-risk neuroblastoma, *Cancer Lett.* 197 (2003) 185–192.
- [57] J.Z. Finklestein, M.D. Krailo, C. Lenarsky, S. Ladisch, G.K. Blair, C.P. Reynolds, et al., 13-cis-Retinoic acid (NSC 122758) in the treatment of children with metastatic neuroblastoma unresponsive to conventional chemotherapy: report from the Childrens Cancer Study Group, *Med. Pediatr. Oncol.* 20 (1992) 307–311.
- [58] S.M. Kumar, S. Liu, H. Lu, H. Zhang, P.J. Zhang, P.A. Gimotty, et al., Acquired cancer stem cell phenotypes through Oct4-mediated dedifferentiation, *Oncogene*. 31 (2012) 4898–4911.
- [59] X. Wang, J. Wang, V. Huang, R.F. Place, L.C. Li, Induction of NANOG expression by targeting promoter sequence with small activating RNA antagonizes retinoic acid-induced differentiation, *Biochem. J.* 443 (2012) 821–828.
- [60] S.K. Thomas, C.A. Messam, B.A. Spengler, J.L. Biedler, R.A. Ross, Nestin is a potential mediator of malignancy in human neuroblastoma cells, *J. Biol. Chem.* 279 (2004) 27994–27999.
- [61] Y.Y. Mahller, J.P. Williams, W.H. Baird, B. Mitton, J. Grossheim, Y. Saeki, et al., Neuroblastoma cell lines contain pluripotent tumor initiating cells that are susceptible to a targeted oncolytic virus, *PLoS One* 4 (2009), e4235.
- [62] J.D. Walton, D.R. Kattan, S.K. Thomas, B.A. Spengler, H.F. Guo, J.L. Biedler, et al., Characteristics of stem cells from human neuroblastoma cell lines and in tumors, *Neoplasia*. 6 (2004) 838–845.
- [63] H. Sartelet, T. Imbriglio, C. Nyalendo, E. Haddad, B. Annabi, M. Duval, et al., CD133 expression is associated with poor outcome in neuroblastoma via chemoresistance mediated by the AKT pathway, *Histopathology*. 60 (2012) 1144–1155.
- [64] S.D. Vangipuram, Z.J. Wang, W.D. Lyman, Resistance of stem-like cells from neuroblastoma cell lines to commonly used chemotherapeutic agents, *Pediatr. Blood Cancer* 54 (2010) 361–368.
- [65] N. Aravindan, D. Jain, D.B. Somasundaram, T.S. Herman, S. Aravindan, Cancer stem cells in neuroblastoma therapy resistance, *Cancer Drug Resist.* 2 (2019) 948–967.
- [66] M.A. Khalil, J. Hrabeta, S. Cipro, M. Stiborova, A. Vicha, T. Eckschlager, Neuroblastoma stem cells - mechanisms of chemoresistance and histone deacetylase inhibitors, *Neoplasma*. 59 (2012) 737–746.
- [67] S. Cipro, J. Hrebackova, J. Hrabeta, J. Poljakova, T. Eckschlager, Valproic acid overcomes hypoxia-induced resistance to apoptosis, *Oncol. Rep.* 27 (2012) 1219–1226.
- [68] W.B. London, R. Bagatell, B.J. Weigel, E. Fox, D. Guo, C. Van Ryn, et al., Historical time to disease progression and progression-free survival in patients with recurrent/refractory neuroblastoma treated in the modern era on Children's Oncology Group early-phase trials, *Cancer*. 123 (2017) 4914–4923.
- [69] Y. Choi, S. Lee, K. Kim, S.H. Kim, Y.J. Chung, C. Lee, Studying cancer immunotherapy using patient-derived xenografts (PDXs) in humanized mice, *Exp. Mol. Med.* 50 (2018) 99.
- [70] A.P. Williams, J.E. Stewart, L.L. Stafman, J.M. Aye, E. Mroczek-Musulman, C. Ren, et al., Corruption of neuroblastoma patient derived xenografts with human T cell lymphoma, *J. Pediatr. Surg.* 54 (2019) 2117–2119.